Transactions of the Korean Nuclear Society Spring Meeting
Chuncheon, Korea, May 25-26 2006

Development of a Fully Implicit Three-Field Solver for Channel Flow

Moonkyu Hwang*, Sung-Won Bae Young-Jin Lee, Bub-Dong Chung
*Korea Atomic Energy Research Institute, P.O. box 150, Yusong-gu, Deajeon, Korea mkhwang@kaeri.re.kr**

1. Introduction

The thermal/hydraulic behavior of the multiphase flow is predicted by solving the related governing equations. The equations are devised based on the mass, momentum, and energy conservation laws and physical models defining the thermal and mechanical interactions between the phases involved. A great deal of efforts has been paid, during the past two or three decades, to solve the equations in an efficient and stable manner. The reliable methodology to obtain the solution of the equation set is essential, especially in nuclear thermal/ hydraulic safety analysis where the consequences of the various hypothetical incidents are required to be within a predefined range of acceptance.

Depending on the method to handle the time derivative term, the methods for solving the mass, momentum and energy equation set are normally categorized as explicit, semi-implicit, and fully implicit methods.

It is well known that the explicit and semi-implicit methods, however, have a shortcoming of the material Courant limit. The maximum allowable time step could be too small for some applications, especially where fine spatial resolutions are required. The separate analysis of the quenching front behavior during the reflood phase of the boil-off accident would be one of such cases. Even though the limitation could be mitigated through SETS method [1] the explicit treatment of the model coefficients between the phases could still limit the allowable time step.

In this study, the fully implicit solver is developed for a one-dimensional channel flow as three-fields. The three-field modeling of the water is also seen in the system codes, as in COBRA [2]. The current work, however, separately treats the thermal energy for the continuous and entrained liquids, as opposed to the combined treatment in COBRA. The separate modeling would allow for a analysis of the thermal interaction of the entrained liquid with highly supper heated steam in a more realistic manner. The higher evaporation might be observed with the separate energy modeling in such a case.

2. Methods

2.1 Governing equations

The governing equation set for the three-field modeling of the two phase flow is based on the time-space average equations of single-pressure two-fluid model [3]. The equations are:

$$\frac{\partial}{\partial t}(\alpha_v \rho_v) + \frac{1}{A}\frac{\partial}{\partial x}(\alpha_v \rho_v v_v A) = \Gamma_v \tag{1}$$

$$\frac{\partial}{\partial t}(\alpha_l \rho_l) + \frac{1}{A}\frac{\partial}{\partial x}(\alpha_l \rho_l v_l A) = -(1-\eta)\Gamma_v - S \tag{2}$$

$$\frac{\partial}{\partial t}(\alpha_e \rho_e) + \frac{1}{A}\frac{\partial}{\partial x}(\alpha_e \rho_e v_e A) = -\eta \Gamma^{''} + S \tag{3}$$

where η stands for the evaporation fraction from the entrained liquid, and the subscription v, l and e are for the vapor, continuous liquid and entrained liquid, respectively. Similarly, the momentum equation and energy equations for the gas phase are, respectively,

$$\begin{aligned}\alpha_v \rho_v \frac{\partial v_v}{\partial t} + \alpha_v \rho_v v_v \frac{\partial v_v}{\partial x} &= -\alpha_v \frac{\partial P}{\partial x} + \alpha_v \rho_v B_x - \tau_{wv} \\ &\quad - \tau_{i,vl} - \tau_{i,ve} + \Gamma_l^{''} v_{I_{vl}} + \Gamma_e^{''} v_{I_{ve}} - \Gamma_v v_v \\ &\quad - C_{v,ve}\alpha_v \alpha_e \rho_{m,ve} \frac{\partial (v_v - v_e)}{\partial t} - C_{v,vl}\alpha_v \alpha_l \rho_{m,vl} \frac{\partial (v_v - v_l)}{\partial t}\end{aligned} \tag{4}$$

$$\begin{aligned}\frac{\partial(\alpha_v \rho_v u_v)}{\partial t} + \left(\frac{1}{A}\right)\frac{\partial (A\alpha_v \rho_v u_v v_v)}{\partial x} &= -P\frac{\partial \alpha_v}{\partial t} - \left(\frac{P}{A}\right)\frac{\partial (A\alpha_v v_v)}{\partial x} \\ &\quad + Q_{wv} + Q_{iv} + \Gamma_{vi} h_g^{*} + \Gamma_w h_g^{'} + DISS_v\end{aligned} \tag{5}$$

The momentum and energy equations for the continuous liquid and entrained liquid can be obtained similarly.

2.2 Finite Difference Equations

The differential equation set is integrated over the 1-diminentional node depicted in Figure 1.

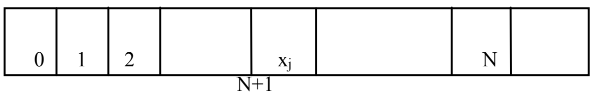

Figure 1. One-dimensional Nodes for a channel flow

The momentum equation for the vapor is in the form of

$$\begin{aligned}&(\alpha_v \rho_v)_{j+1/2}^{n+1} \frac{(v_v)_{j+1/2}^{n+1} - (v_v)_{j+1/2}^{n}}{\Delta t} A_{j+1/2}\Delta x_{j+1/2} + \\ &\langle(\alpha_v \rho_v v_v) v_v\rangle_{j+1}^{n+1} A_{j+1} - \langle(\alpha_v \rho_v v_v) v_v\rangle_{j}^{n+1} A_j \\ &= -(\alpha_v)_{j+1/2}^{n+1}\left(P_{j+1}^{n+1} - P_j^{n+1}\right)A_{j+1/2} \\ &\quad + \begin{bmatrix}(\alpha_v \rho_v B_x)_{j+1/2}^{n+1} - (\tau_{wv})_{j+1/2}^{n+1} - (\tau_{i,vl})_{j+1/2}^{n+1} - (\tau_{i,ve})_{j+1/2}^{n+1} \\ -(\Gamma_E)_{j+1/2}^{n+1}(v_v)_{j+1/2}^{n+1} + (1-\eta_{j+1/2}^{n+1})(\Gamma_E)_{j+1/2}^{n+1}(v_l)_{j+1/2}^{n+1} \\ +\eta_{j+1/2}^{n+1}(\Gamma_E)_{j+1/2}^{n+1}(v_e)_{j+1/2}^{n+1} - (F_{vl}^{VM})_{j+1/2}^{n+1} - (F_{ve}^{VM})_{j+1/2}^{n+1}\end{bmatrix} A_{j+1/2}\Delta x_{j+1/2}\end{aligned} \tag{6}$$

The advection terms enclosed in the angle bracket $\langle\ \rangle$ are evaluated as an upwind scheme. The mass, and energy equations as well as the momentum equations for other fields are derived similarly. As seen in the equations (6), all the terms on the right side are evaluated at the time step of (n+1), meaning the scheme is treated fully-implicitly.

2.3 Solving the Finite Difference Equations Set

The total of nine equations for the whole governing equation set is solved by Newton iteration [4,5].

For the system of equations

$$f_i(x_1,\ldots,x_n)=0, \qquad i=1,\ldots,n. \qquad (7)$$

To obtain the solution $\bar{x}=(x_1,\ldots,x_n)^T$, let $\bar{x}^*$ be the true solution of the equation set (7) and $\bar{x}^0$ be the guess for this solution. Then we expand each function f_i about $\bar{x}^0$ as:

$$f_i(\bar{x}) \doteq f_i(\bar{x}^0)+\sum_{j=1}^{n}\frac{\partial f_i}{\partial x_j}(\bar{x}^0)(x_j-x_j^0)\equiv l_i(\bar{x}) \qquad (8)$$

Then, we solve $l_i(\bar{x})=0, i=1,\ldots,n$ to obtain the new approximation $\bar{x}^1$ to $\bar{x}$. The process is repeated until a convergence conditions are satisfied. The process can be represented as a matrix form of

$$\bar{F}'(\bar{x}^m)(\bar{x}^{m+1}-\bar{x}^m)=-\bar{F}\ (\bar{x}^m) \qquad (9)$$

The essential step in equation (9) is to determine the derivative $F'(\bar{x}^m)$ which is

$$\bar{F}'(\bar{x}^m)=\frac{\partial\bar{F}}{\partial\bar{x}^m}=\bar{\bar{J}}^m \qquad (10)$$

The each element of the Jacobian matrix is determined using the numerical differentiation

3. Results and Discussion

The fully-implicit set of finite deference equation implemented using the Newton iteration is tested. Although the interphase phenomena modeling is not completed at this stage of development, the soundness of the solver is verified by the following tests. In test 1, the motion of the liquid phase is calculated in the vertical channel without a wall friction. The free-fall behavior with the equilibrium pressure boundary condition is verified by the velocity of 9.8m/s and 19.6m/s at time=1sec and 2sec, respectively, with 5 digit accuracy. The second test is pressure wave test with a slightly elevated pressure of 1.1 bar initiated at one end of a channel filled with a liquid water at 1.0 bar. The channel is modeled with 20 nodes. The pressure variations are seen in the figure 2 for 2 meter and 10 meter channels. The 10 meter channel is seen to require more time to damp out the pressure wave.

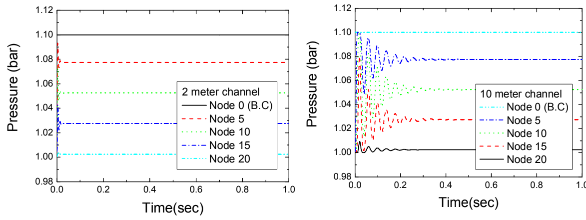

Figure 2. Pressure shock waves

The last test is a manometer problem. The U-tube modeling and the velocity change at the node 10 is depicted in Figure 3. The liquid which initially occupies nodes 5 to 18 is released at time 0.0, resulting manometer oscillation driven by the gravity force. The amplitude of the velocity is seen to reduce very slightly. The pressure variances for node 2 to 6 are seen to be very stable too.

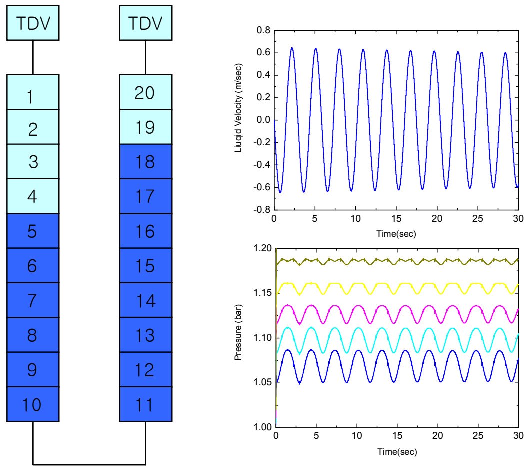

Figure .3 Manometer nodding with velocity and pressures

4. Summary

In this study, a fully implicit solver for the two phase flow is developed. The two phase flow of water is modeled by three field mass, momentum and energy equation set. The initial verification tests show good physical consistency. With the closure laws for the interphase interactions, which are under development, the fully implicit solver is expected as a viable tool for developing and examining the key phenomena in the two phase channel flow.

REFERENCES

[1] Mahaphy, J.H., A stability-enhancing two-step method for fluid flow calculations. J. Comp. Phys 46, 329-241 (1982)

[2] Paik, C.Y., et. al., Analysis of FLECHT-SEASET 163-Rod blocked Bundle Data using COBRA-TR, NUREG/CR-4166

[3] Ishii, M. and Mishma, Two-fluid model and hydrodynamic constitutive relations. Nucl. Eng. Des. 82. 107-126 (1982)

[4] Golub, G., Scientific Computing, An Introduction With Parallel Computing, Academic Press, Inc. (1993)

[5] Frepoli, C., et.al., Note of the implementation of a fully-implicit numerical scheme for a two-phase three-field flow model, Nucl. Eng. Des. 225, 191-217 (2003)